

Short-period AM CVn systems as optical, X-ray and gravitational wave sources

G. Nelemans^{1*} and L. R. Yungelson^{2,3} and S.F. Portegies Zwart⁴

¹*Institute of Astronomy, University of Cambridge, Madingley Road, Cambridge CB3 0HA, UK*

²*Institute of Astronomy of the Russian Academy of Sciences, 48 Pyatnitskaya Str., 109017 Moscow, Russia*

³*Isaac Newton Institute, Moscow Branch, 13 Universitetskii pr., 119899, Moscow, Russia*

⁴*Astronomical Institute “Anton Pannekoek” and Section Computational Science, University of Amsterdam, Kruislaan 403, NL-1098 SJ Amsterdam, the Netherlands*

Accepted . Received 12 September 2018

ABSTRACT

We model the population of AM CVn systems in the Galaxy and discuss the detectability of these systems with optical, X-ray and gravitational wave detectors. We concentrate on the short period ($P < 1500$ s) systems, some of which are expected to be in a phase of direct impact accretion. Using a self-consistent model for the star formation history and radial distribution of stars in the Galaxy plus simple models for the emission of optical and X-ray radiation from the AM CVn systems and interstellar absorption, we derive the sample of short-period AM CVn systems that can be detected in the optical and/or X-ray bands. At the shortest periods the detectable systems are all X-ray sources, some with periods as short as three minutes. At periods above 10 minutes most detectable systems are optical sources. About one third of the X-ray sources are also detectable in the optical band. We also calculate the gravitational wave signal of the short-period AM CVn systems. We find that potentially several thousand AM CVn systems can be resolved by the gravitational wave detector *LISA*, comparable to the expected number of detached double white dwarfs that can be resolved. We estimate that several hundreds of the AM CVn systems resolvable by *LISA*, are also detectable in the optical and/or X-ray bands.

Key words: gravitational waves – binaries: close – white dwarfs

1 INTRODUCTION

AM CVn systems are binaries, with periods less than 1 hour, in which a white dwarf accretes matter from a low-mass, helium-rich, object. The mass transfer is driven by gravitational wave radiation (e.g. Paczyński 1967). They are observed at optical wavelengths as faint blue and variable objects. For a reviews of observational work on AM CVn systems, see Warner (1995); Solheim (2003). A discussion of the formation and modelling of the population can be found in Tutukov & Yungelson (1996), Nelemans et al. (2001a), hereafter NPVY and Podsiadlowski, Han & Rappaport (2003). Hils & Bender (2000) and Nelemans, Yungelson & Portegies Zwart (2001b) discussed the contribution of the AM CVn population to the Galactic unresolved gravitational wave background.

The number of known or suspected systems is rapidly increasing: six new (candidate) AM CVn systems have been found in the last five years: CE 315, with a period of 65.1 minutes (Ruiz et al. 2001); KL Dra, with a period of 25 minutes (Jha et al. 1998; Wood et al. 2002); “2003aw”, with a possible period of 34 minutes

Woudt & Warner (2003b); RX J1914.4+2456 (V407 Vul), with a period of 9.5 minutes (Cropper et al. 1998; Ramsay et al. 2000; Ramsay et al. 2002b; Marsh & Steeghs 2002), KUV 01584–0939 (ES Cet) with a period of 10.3 minutes (Warner & Woudt 2002) and RX J0806.3+1527 with a period of 5.3 minutes (Israel et al. 2002; Ramsay et al. 2002a). RX J1914.4+2456 and RX J0806.3+1527 were discovered as *ROSAT* X-ray sources (Motch et al. 1996; Israel et al. 1999). For these two systems the interpretation as AM CVn systems has been questioned (Wu et al. 2002; Norton et al. 2002), but not for the other four new systems.

The last three of the new systems mentioned above are particularly interesting as theoretical models of the evolution of AM CVn systems and their current Galactic population (e.g. Tutukov & Yungelson 1996, NPVY) show that the expected number of systems at periods shorter than ~ 10 minutes is small, and an optically selected sample will be dominated by longer period systems. However, at these short periods the mass transfer rate is as high as $10^{-6} - 10^{-8} M_{\odot} \text{ yr}^{-1}$, and therefore systems might be discovered as X-ray, rather than optical sources, as is the case for the two *ROSAT* sources. At these short periods the systems are also promising sources for low-frequency gravitational wave (GW) detectors (e.g. Israel et al. 2002; Marsh & Steeghs 2002).

* E-mail: nelemans@ast.cam.ac.uk

In this paper we determine the range of orbital periods in which AM CVn systems could be discovered as X-ray sources, using simple, average temperature and blackbody emission models and taking into account interstellar absorption. We estimate the number of such systems in the Galaxy and their brightness in the optical band. We compute the number of short-period ($P < 1500$ s) AM CVn systems that could be detected by the planned low-frequency gravitational wave radiation (GWR) detector in space, *LISA*, and focus on the subset of these systems that are expected to have optical and/or X-ray counterparts, as combined observations will lead to a better understanding of the physical state, formation and population of AM CVn systems. We will use the term “AM CVn system” throughout the paper for all double-degenerate interacting binaries with helium secondaries, irrespective of their optical properties.

In Sect. 2 we review our Galactic model of AM CVn systems, discuss the changes we made with respect to NPVY and the uncertainties in this model. The emission of optical, X-ray and gravitational wave signals from AM CVn systems is discussed in Sect. 3. The selection effects and the resulting expected population of sources detectable in the optical and X-ray bands, and as GWR sources are presented in Sect. 4. In Sect. 5 we consider the *LISA* sources that have optical and/or X-ray counterparts. Discussion (Sect. 6) and conclusions (Sect. 7) follow.

2 A MODEL FOR THE CURRENT GALACTIC POPULATION OF AM CVn SYSTEMS

2.1 Formation of AM CVn systems

For a detailed discussion of the formation of AM CVn systems we refer to NPVY, and references therein, so here we only give a brief summary. There are two main routes for the formation of AM CVn systems: (i) via a phase in which a double white dwarf loses angular momentum due to gravitational wave radiation and evolves to shorter and shorter periods to start mass transfer at periods of a few minutes and (ii) via a phase in which a non-degenerate helium star transfers matter to a white dwarf accretor.

Recently Podsiadlowski et al. (2003) proposed a third scenario to form AM CVn binaries, similar to the usual scenario for the formation of cataclysmic variables (CVs), via a phase of mass transfer in the course of which a low-mass star with initially almost exhausted hydrogen core or a small helium core becomes a helium white dwarf¹. We found that with the assumptions used in this paper (see below) this scenario is relatively unimportant for the short-period systems discussed here (giving less than two per cent of the systems), so for the remainder of the paper we leave it out of our model, but briefly come back to it in the discussion (Sect. 6).

One of the main conclusions of NPVY was that the uncertainties in the models for the formation of AM CVn systems resulted in widely varying numbers of expected systems in the Galaxy. The most optimistic and most pessimistic cases of NPVY gave roughly 80 and 18 million systems in the Galaxy at present. The uncertainty is particularly severe for the shortest period AM CVn systems, which probably have to form through the double white dwarf scenario. In NPVY we showed that at the start of the mass transfer between double white dwarfs there is a phase of “direct impact accretion”, in which the gas stream flowing from the donor to the

¹ Such a scenario has been proposed before (e.g. Tutukov et al. 1987) as a formation scenario for ultra-compact X-ray binaries

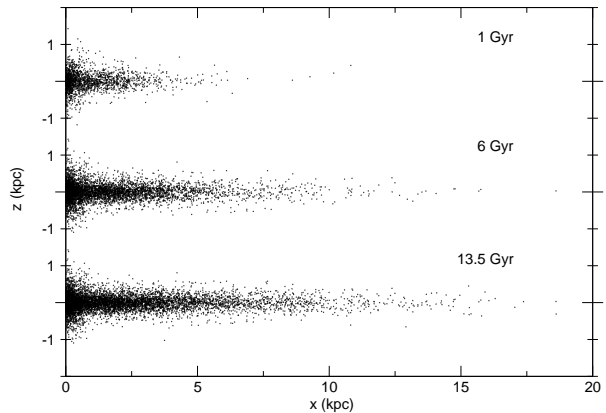


Figure 1. The distribution of stars in the $x - z$ plane of the Galaxy for our implementation of the Boissier & Prantzos (1999) model at Galactic ages of 1, 6 and 13.5 Gyr, using a number of tracer particles proportional to the total mass in stars (M_*) in the Galaxy as indicated in the plot. The change in the radial extent of the star forming region in time is clearly visible. For the total SFR as function of time, see Fig. 2.

accretor hits the accretors surface directly without forming an accretion disc (see also Webbink 1984). In this phase the stability of the mass transfer depends crucially on the tidal (or other) coupling between the spin of the accretor and its companion (NPVY, see for a detailed discussion of the stability Marsh, Nelemans & Steeghs 2003).

The formation of systems formed via the helium star scenario is also uncertain because of the possibility of so called edge-lit-detonation (ELD) of the accreting white dwarf before the system reaches the AM CVn phase (see NPVY). In the current study we use the most optimistic model (Model II of NPVY), in which we assume efficient coupling in the direct impact phase, and that accretion of at least $0.3 M_{\odot}$ of He is necessary for ELD. But we note that recent calculations, including rotation, of helium accreting white dwarfs suggest that ELD might not happen at all (Yoon & Langer 2003). This would increase the formation rate of AM CVn systems via the helium star scenario in our most optimistic model by about 15 per cent. For the short period systems discussed here the total uncertainty is probably of the order of a factor 10 at least.

We note that we do not take into account the unstable helium burning on the surface of carbon-oxygen white dwarfs accreting helium at high rates and the possible associated mass loss (see, e.g. Kato & Hachisu 1999).

2.2 Galactic model, star formation history and stellar evolution

Instead of the simple Galactic model we used before, we implemented a star formation rate (SFR) as function of time and position in the Galaxy based on the model of Boissier & Prantzos (1999). We obtain the SFR as function of R and t by linear interpolation between values in a table (S. Boissier, private communication), and assume that the probability of a star being born with a radius R or smaller goes with the integrated SFR, i.e.

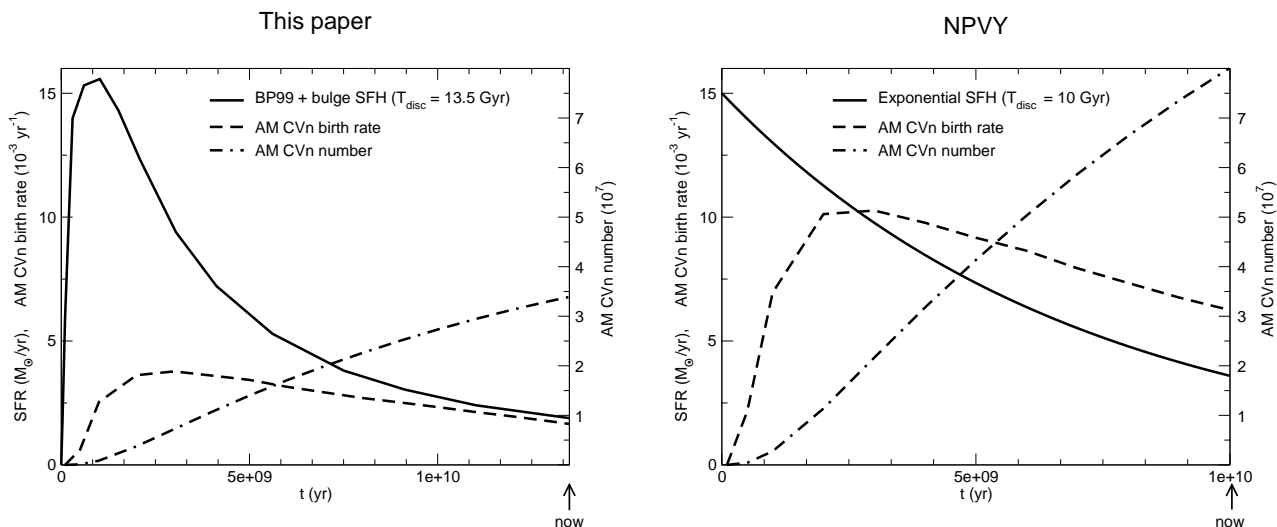


Figure 2. Illustration of the difference in Galactic model between the current work (left panel) and NPVY (right panel). Shown are the SFR (solid lines), the birth rate of AM CVn systems (dashed line, left ordinate), and their total number (dot-dashed line, right ordinate) as function of time in the Galaxy. The differences in the birth rate and number of AM CVn systems reflect the differences in star formation history and the treatment of stellar evolution (see Sect. 2.3). Note that in the exponential model the Galactic age is 10 Gyr, while the Boissier & Prantzos (1999) model has an age of 13.5 Gyr.

$$P(R, t) = \frac{\int_0^R \text{SFR}(R', t) 2\pi R' dR'}{\int_0^{R_{\max}} \text{SFR}(R', t) 2\pi R' dR'}, \quad (1)$$

where R_{\max} is the maximum extent of the disc (19 kpc) and we assume that the stars do not migrate radially in time. The age of the Galaxy in this model is 13.5 Gyr. As the Boissier & Prantzos (1999) model gives the SFR projected onto the plane of the Galaxy, we assume a z -distribution,

$$P(z) \propto \text{sech}(z/z_h)^2, \quad (2)$$

as in Nelemans et al. (2001c), where $z_h = 200$ pc, neglecting its age and mass dependence. We have added a bulge to the model, simply by doubling the SFR in the inner 3 kpc of the Galaxy compared to Boissier & Prantzos (1999). As a result the total mass in this region is $2.6 \cdot 10^{10} M_{\odot}$ at the current age of the Galaxy, consistent with kinematic and micro-lensing results (e.g. Klypin et al. 2002). We distribute the stars in the bulge according to

$$\rho_{\text{bulge}} = \exp(-(r/0.5 \text{ kpc})^2), \quad (3)$$

where $r = \sqrt{x^2 + y^2 + z^2}$.

In Fig. 1 we plot the resulting distribution of stars in the $x - z$ plane of the Galaxy, showing the z -distribution of stars and the change in the radial extent of the star formation as function of time. For the SFR integrated over R as function of time, see Fig. 2 (left panel).

The important effect resulting from the different choice of Galactic model is that for most of the time in the Galactic history, the SFR is lower in the Boissier & Prantzos (1999) model than in the ‘exponential’ model used in NPVY (see Fig. 2); in particular, the current SFR is lower than the one we obtained previously (1.9 vs $3.6 M_{\odot} \text{ yr}^{-1}$). This has a strong effect on the current birth rates of AM CVn systems, since the latter follow star formation history with a typical delay of several Gyr (Tutukov & Yungelson 1996; Nelemans et al. 2001a). However, the integrated SFR remains quite similar (8.2×10^{10} vs. $8 \times 10^{10} M_{\odot}$), partly due to the different Galactic ages (13.5 vs. 10 Gyr). Another characteristic of our new

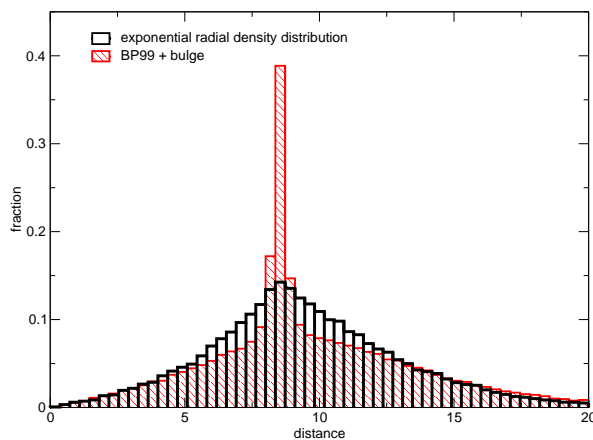


Figure 3. Histogram of distances to the Earth of short period AM CVn systems for our implementation of the Boissier & Prantzos (1999) model with added bulge and for an exponential radial density distribution.

model is that the Galactic distribution is more centrally concentrated than with an exponential radial density distribution, mainly due to the inclusion of the bulge. In Fig. 3 we show the distribution of distances from the Earth of the population of short-period AM CVn systems in the Galaxy for the two models. The concentration in the Galactic centre with the new model is clearly visible. As the longer period AM CVn systems are older, their distribution is even more centrally concentrated

Another new element in our current study is the use of the IMF as proposed by Kroupa, Tout & Gilmore (1993), rather than the Miller & Scalo (1979) IMF as used in NPVY. Because the Kroupa et al. (1993) IMF is steeper for masses above $1 M_{\odot}$, the same star formation history leads to fewer AM CVn systems, especially for the helium star formation scenario, the efficiency of which is reduced by about 25 per cent (see Sect. 2.3).

Formation channel	birth rate (10^{-3} yr^{-1})	total number (10^7)
double white dwarfs	1.3	2.3
helium stars	0.27	1.1
total	1.6	3.4

Table 1. Present day birth rates and total number of AM CVn systems in the Galaxy in our current model, for the different formation channels.

We use the population synthesis code **SeBa**, developed by Portegies Zwart & Verbunt (1996, see also Nelemans et al. 2001c). We assume a 50 per cent binary fraction, an initial distribution of separations in binary systems (a) flat in $\log a$ between contact and $10^6 R_{\odot}$, a flat mass ratio distribution and a thermal eccentricity distribution.² The current study is based on a model with 250,000 ZAMS binaries. For the treatment of the stellar evolution and the mass transfer we refer to our earlier papers, but recall that we use a common envelope formalism based on the angular momentum balance for the first episode of unstable mass transfer in the system, as detailed in Nelemans et al. (2000, 2001c). Two small changes that turn out to be important are in the formation and evolution of white dwarfs. We updated our treatment of the growth of the core in giants as described in Nelemans et al. (2001c), by including a simple model of the second dredge-up to be more in line with detailed stellar evolution models (e.g. Hurley et al. 2000). The second change is in the treatment of white dwarf cooling (see Appendix A) and white dwarf mass – radius relation, for which we now use the fit by Eggleton, as given in Verbunt & Rappaport (1988), rather than the Zapolsky & Salpeter (1969) relation, which is not appropriate for massive white dwarfs.

The last change we made compared to NPVY is in the maximum rate at which a main sequence star can accrete before it expands and mass will be lost from the system. We used to limit this to accretion at the thermal time scale of the accretor. However, as is shown e.g. by Kippenhahn & Meyer-Hofmeister (1977), higher accretion rates do not necessarily lead to expansion of the accretor. We therefore use the treatment of Pols & Marinus (1994) which takes the reaction of the radius of the accreting star upon mass gain into account.

2.3 Total population of AM CVn systems in the Galaxy

With the changes described in the previous section, we obtain, for the two formation channels discussed here, the current birth rates and total number of AM CVn systems in the Galaxy as shown in Table 1 and Fig. 2 (compare Table 1 in NPVY). The difference between the numbers presented here and in NPVY are due to the use of the new Galactic mode, different IMF and the changes in the treatment of stellar evolution described in Sect. 2.2. All these change the birth rate of AM CVn systems at any time, e.g. at the current Galactic age the birth rate of the white dwarf family goes down by ~ 60 per cent due to the Galactic model and is reduced further by another ~ 40 per cent due to the changes in treatment of white dwarf formation and mass – radius relation. The birth rate of

² All binaries discussed here will be circularized to somewhat smaller separation before the first phase of mass transfer and thus the shape of the initial eccentricity distribution hardly influences the number of AM CVn systems.

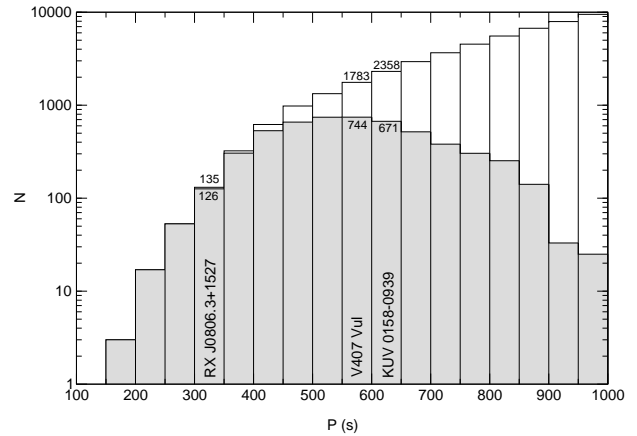


Figure 4. Histogram of periods of the shortest period AM CVn systems. The shaded histogram gives the number of systems which are in the direct impact phase (but note the logarithmic y-scale). The observed systems are indicated at their suggested orbital periods. The number of systems in these bins are indicated.

the helium star family goes down by ~ 60 per cent due to the Galactic model, ~ 25 per cent due to the IMF and ~ 40 per cent due to the higher accretion rate limit for main-sequence stars (because less systems pass through common envelopes and become close enough to produce AM CVn systems). Partly compensated by the change in the age of the Galaxy this results in 55 and 65 per cent fewer systems present in the Galaxy for the two families, respectively.

In Fig. 4 we show a histogram of the shortest period systems as function of orbital period, indicating the systems in the direct impact phase and the periods of the observed (candidate) AM CVn systems.

3 MODELLING THE OPTICAL, X-RAY AND GW EMISSION OF AM CVn SYSTEMS

In order to be able to compare our results with (future) observations we have to simulate the emission produced by our model systems. We determine the temperature and luminosity of the different emission sources and determine how much energy is emitted in a certain band, assuming the emitted spectrum is a blackbody. For the present study we only discuss emission in V -band and the *ROSAT* 0.1–2.4 keV X-ray band plus gravitational wave radiation. We chose the *ROSAT* band, because the two candidate systems were found as *ROSAT* sources and because we can compare our results to the *ROSAT* all-sky survey. However, in Sect. 6 we briefly discuss the expected results for the *Chandra* and *XMM*.

There are four main emission sites: the accretion disc and boundary layer between disc and accreting white dwarf, the impact spot in the case of direct impact accretion, the accreting star and the donor star.

3.1 Optical emission

The disc. We assume that half of the accretion luminosity is radiated by the disc (the other half in the boundary layer), i.e.

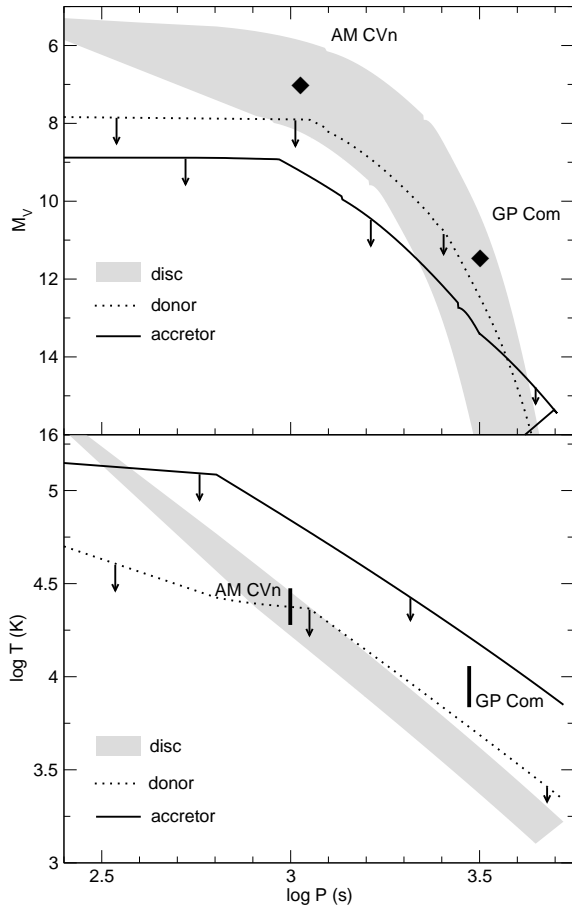


Figure 5. Absolute magnitudes and temperatures of the different optical emission components as function of orbital period. The limits of the regions are defined by systems with initial masses of $0.15 + 0.25 M_{\odot}$ and $0.3 + 1.0 M_{\odot}$. For the accretor and donor we give the upper limits on the magnitude and temperature for the extreme case that the donor/accretor white dwarf was young and hot at the start of the AM CVn phase, i.e. at the top of the cooling curve (see Appendix A).

$$L_{\text{disc}} = \frac{1}{2} G M \dot{m} \left(\frac{1}{R} - \frac{1}{R_{L1}} \right) \text{erg s}^{-1}, \quad (4)$$

where M and R are the mass and radius of the accretor and R_{L1} is the distance of the first Lagrangian point to the centre of the accretor and \dot{m} is the mass transfer rate. Because the two white dwarfs are so close together the usual assumption that the matter falls in from infinity is not valid (Han & Webbink 1999). We model the optical emission from the disc like in NPVY, according to Wade (1984), as a single temperature disc that extends to 70 per cent of the Roche lobe of the accretor, radiates as a blackbody and use the bolometric correction appropriate for its temperature.

The donor. We model the emission from the donor as the cooling luminosity of the white dwarf, using approximations to the models of Hansen (1999), see the Appendix A.

The accretor. We model the emission from the accretor as being the unperturbed cooling luminosity of the white dwarf.

In our simple model we do not take into account such effects as irradiation of the donor by the impact spot or disc, heating of the accretor by radiation from the disc/boundary layer (e.g. Pringle

1988), compressional heating (e.g. Townsley & Bildsten 2002) or tidal heating of the two white dwarfs prior to contact (Iben et al. 1998).

In Fig. 5 we show the range of absolute V -magnitudes (M_V) and temperatures of the different optical components described above, for systems forming from double white dwarfs. The top panel shows the range of absolute magnitudes of the discs as function of period (in grey). The two symbols show the observed absolute magnitudes for AM CVn and GP Com [using distances of 235 pc for AM CVn (C. Dahn³, private communication) and 70 pc for GP Com (Thorstensen 2003)], while the bars in the bottom panel show the range of effective temperatures for these systems. The upper and lower limit of the shaded regions are for two combinations of masses that bracket the range of masses of the majority of the systems: $0.3 + 1.0$ and $0.15 + 0.25 M_{\odot}$ respectively.

Because for the accretor and donor we assume that their luminosity is the cooling luminosity, their magnitudes depend on their ages, rather than on the orbital period. However, during the AM CVn phase there is a direct relation between time and period (e.g. figure 4 in NPVY) so for given cooling luminosity at the start of the mass transfer we can plot the magnitude of the cooling white dwarf as function of orbital period. In Fig. 5 we plot that curve for the extreme case in which the cooling luminosity at the starts of the mass transfer is that of a newly born, very hot and luminous white dwarf. In reality the donor and accretor are typically of the order of a Gyr old, so they evolve along a track that lies below these curves. Towards the longer periods, the age of the system is a few Gyr anyway, so the curves for all initial luminosities converge.

The few observed systems fall in the grey area in Fig. 5 indicating that our simple model is at least able to understand these systems satisfactorily except the temperature of GP Com⁴. The same model can be adopted for the systems that form via the helium-star donors. In these cases, however, the curves shift to longer periods (see NPVY).

3.2 X-ray emission

In modelling the X-ray emission of AM CVn systems we distinguish two cases: with and without disc.

If there is no disc, the gas stream hits the companion directly and a small area of the surface will be heated. We assume that the full accretion luminosity is radiated as a blackbody with a temperature given by

$$\left(\frac{T_{\text{BB}}}{T_{\odot}} \right)^4 = \frac{1}{f} R^{-2} L_{\text{acc}}, \quad (5)$$

where L_{acc} and R are in solar units and L_{acc} is defined by Eq. (4). The fraction f of the surface that is radiating depends on the details of the accretion, but will in general be small. We used $f = 0.001$, which is consistent with the observed X-ray emission of V407 Vul and simple arguments regarding the impact stream (Marsh & Steeghs 2002).

If there is an accretion disc, the X-ray emission can come from the boundary layer between the inner disc and the accretor, where we assume half of the accretion luminosity is radiated, as suggested e.g. by Pringle (1977), or it might have a non-thermal

³ On behalf of the USNO CCD Parallax Team.

⁴ Indeed the continuum emission of GP Com originates at the reheated accreting white dwarf, rather than in the disc (see Bildsten et al., in preparation).

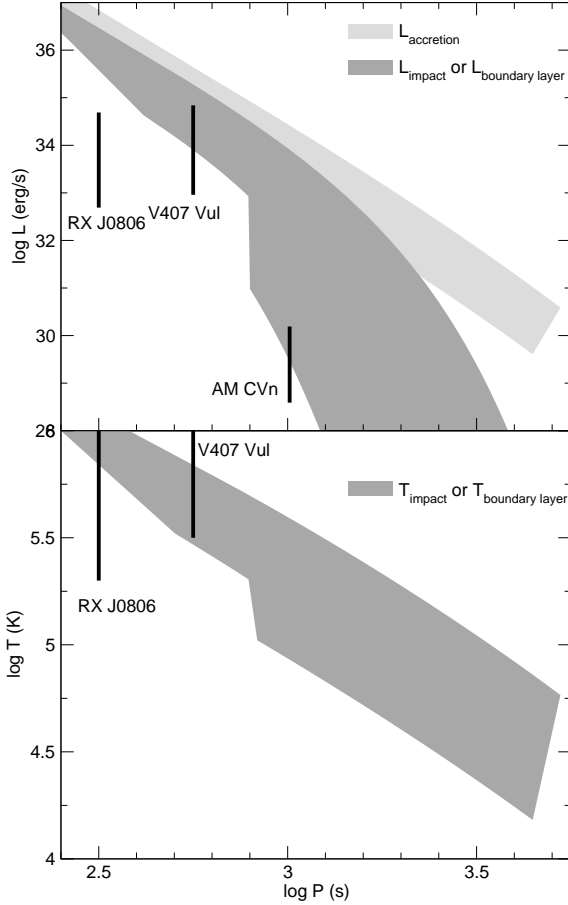


Figure 6. Total accretion luminosity and luminosity and temperatures of the X-ray emission components (impact spot or boundary layer) as function of orbital period. The limits of the regions are again defined by systems with initial masses of $0.15 + 0.25 M_{\odot}$ and $0.3 + 1.0 M_{\odot}$.

origin. The average temperature of the disc (Wade 1984), which we use to estimate the optical emission is never high enough to produce X-rays (Bath et al. 1974). Even though from observations of cataclysmic variables it is clear that the real X-ray emission mechanism is much more complicated (e.g. Hoare & Drew 1991; Mauche et al. 1991; van Teeseling & Verbunt 1994; van Teeseling et al. 1996), we model the X-ray emission of systems with a disc for the moment as coming from the boundary layer, with temperature (Pringle 1977)

$$T_{\text{BL}} = 5 \times 10^5 \left(\frac{\dot{m}}{10^{18} \text{ g/s}} \right)^{\frac{2}{9}} \left(\frac{M}{M_{\odot}} \right)^{\frac{1}{3}} \left(\frac{R}{5 \times 10^8 \text{ cm}} \right)^{-\frac{7}{9}} \text{ K.} \quad (6)$$

In Fig. 6, top panel, we show how the luminosity in X-rays compares to the total accretion luminosity. For the X-ray luminosity we consider here the emission in the *ROSAT* band, from 0.1 – 2.4 keV. The temperature of the impact spot or boundary layer is shown in the bottom panel. The sharp drop in the X-ray luminosity and temperature at the bottom of the darker region at $\log P \approx 2.9$ is caused by the change from direct impact to disc accretion in the low-mass system. We assume that the transition from the impact temperature to the boundary layer temperature is instantaneous. This transition for the more massive system occurs just left off the

plot, where the evolution is so fast that hardly any systems are expected to be observed.

At periods larger than 1000 – 2000 s the mass transfer rates drop to below $10^{-10} M_{\odot} \text{ yr}^{-1}$, the temperature drops below 10^5 K and hardly any X-ray emission is produced in the boundary layer. The inferred temperatures and X-ray luminosities of RX J0806 and V407 Vul are plotted as the bars in the figures. For RX J0806, we use the X-ray flux ($4 \times 10^{-10} \text{ erg cm}^{-2} \text{ s}^{-1}$), distance (0.1 – 1 kpc) and blackbody temperature ($6^{+13}_{-4} \times 10^5 \text{ K}$) as given by Israel et al. (2002). For V407 Vul blackbody temperatures of 43 and 56 eV are derived by Motch et al. (1996) and Ramsay et al. (2002b) respectively, while the latter authors derive an X-ray luminosity of $1.2^{+4.1}_{-0.3} \times 10^{33} \text{ erg s}^{-1}$, for a distance of 100 pc and we plot these limits for a distance range 100 – 400 pc (Ramsay et al. 2000). The X-ray luminosity of AM CVn is taken from Ulla (1995). Except for the luminosity of RX J0806, our very simple model agrees well with the observations.

3.3 Gravitational wave emission

We assume that AM CVn systems emit GWR as two point sources, i.e. neglecting any effect of the deformation of the donor, which fills its Roche lobe and the mass in the accretion disc, if present (see Rezzolla et al. 2001, for a discussion of the small effect of deformation for cataclysmic variables). The amplitude of the GWR signal, as can be detected by *LISA*, is given by (e.g. Evans et al. 1987)

$$h = 0.5 \times 10^{-21} \left(\frac{\mathcal{M}}{M_{\odot}} \right)^{5/3} \left(\frac{P_{\text{orb}}}{1 \text{ hr}} \right)^{-2/3} \left(\frac{d}{1 \text{ kpc}} \right)^{-1}, \quad (7)$$

where $\mathcal{M} = (Mm)^{3/5}/(M+m)^{1/5}$ is the chirp mass, P_{orb} is the orbital period and d is the distance to the system.

4 RESULTS I: THE DETECTABLE POPULATION OF SHORT-PERIOD AM CVn SYSTEMS

4.1 Selection effects

To compare our models with the number of observed systems, we have to decide which of the model systems would be detectable.

For the optical emission we focus on model systems that are brighter than $V = 20$ mag, which is similar to the optical magnitude of the observed short period AM CVn candidates. To take the interstellar reddening into account we use the Sandage (1972) model

$$A_V(\infty) = 0.165 \frac{(\tan(50^\circ) - \tan(b))}{\sin(b)} \quad \text{for } b < 50^\circ \\ = 0 \quad \text{for } b \geq 50^\circ, \quad (8)$$

and $A_V(d)$ follows from our Galactic model [Eq. (2)]

$$A_V(d) = A_V(\infty) \tanh \left(\frac{d \sin(b)}{z_h} \right). \quad (9)$$

For the sources detectable in X-rays we select the systems with an X-ray flux in the 0.1 – 2.4 keV (*ROSAT*) band higher than $10^{-13} \text{ erg s}^{-1} \text{ cm}^{-2}$. To estimate this flux we use the intrinsic flux in this band (Sect. 3.2), the distance and an estimate of the Galactic hydrogen absorption (Morrison & McCammon 1983). We modelled the hydrogen column density after Predehl & Schmitt (1995) as

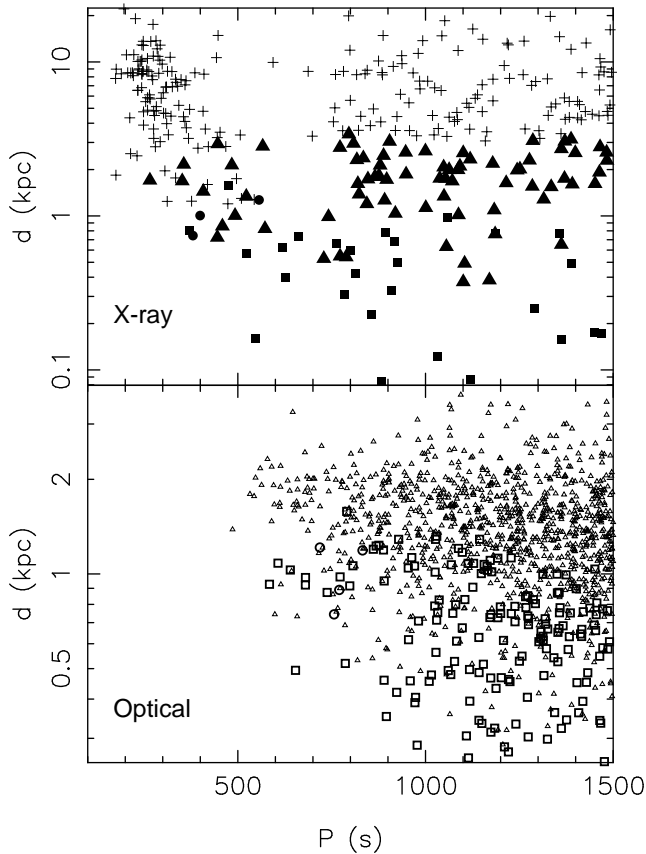


Figure 7. Period vs distance distribution of systems detectable in the X-ray and/or optical bands. **Top panel:** Systems detectable only in X-rays (pluses), and systems that are detectable in the optical and X-ray band (filled circles: direct impact systems with a bright donor, filled triangles: systems with an optically bright disc, filled squares: systems with bright disc + donor). **Bottom panel:** Systems only detectable in the optical band (circles: direct impact systems with a bright donor, triangles: bright discs, squares: bright disc + donor).

$$N_H = 0.179 A_V(d) 10^{22} \text{ cm}^{-2}. \quad (10)$$

4.2 Systems detectable in the optical and X-ray bands

In Fig. 7 we show the sample of the systems that would be detectable in the optical and/or X-ray bands, taking into account the selection effects described above. The relevant numbers are given below in the text, between square brackets (see also Table 3). (We should recall that the results we discuss represent one possible random realization of the model for current Galactic population of AM CVn systems, so all numbers given are subject to Poisson noise). We limited ourselves to the short period systems, with $P < 1500$ s. At longer periods the optical emission from the disc will completely dominate and the detectable sample has been discussed in NPVY. Fig. 7, top panel, shows the systems detectable in X-rays. Pluses are [220] systems only detectable in X-rays, while the filled symbols mark systems also detectable in the V-band.

At the shortest periods a significant fraction of the small number of systems that exist (see Fig. 4) produces enough X-rays that they are detectable even though the sources are close to the Galactic centre (Fig. 7). At longer periods the X-rays get weaker (and softer) so only the systems close to the Earth can be detected. Several of these systems are also detectable in the optical band (filled

symbols). The [3] filled circles show the systems in the direct impact phase, where the optical emission comes solely from the donor as the impact spot is too hot to emit in the V-band. Systems with optical emission from a disc are shown as triangles [75]. There are some [28] systems that are close enough to the Earth that the donor stars can be seen as well as the discs (filled squares). Above 600 s the systems descending from helium star donors appear and have high enough mass transfer rate to be X-ray sources, the closer ones also being visible in the V-band (filled triangles/squares, as these systems always have a disc).

The X-ray sources at larger distances (pluses) are almost all in the bulge and thus are concentrated in a small area on the sky. The closer systems, which often are also detectable in the V-band are more evenly distributed over the sky.

The bottom panel of Fig. 7 shows the 1230 ‘classical’ AM CVn systems, detectable only by the optical emission, for most systems only from their accretion disc (open triangles [1057]). Of this population the ones closest to the Earth in some cases [169] also have a visible donor (open squares). A few [4] direct impact systems only have a visible donor, but are not X-ray sources (open circles). The majority of the optically detectable systems represented in the lower panel of Fig. 7 (with orbital periods between 1000 and 1500 s) are expected to show outbursts due to the viscous-thermal disc instability (Tsugawa & Osaki 1997) which could enhance the chance of their discovery.

Comparing these results with the tentative classification of V407 Vul and RX J0806 as direct impact systems, detectable in X-rays and (just) in the optical band, shows that a few of such systems (filled circles) could be expected in the Galaxy, given all the uncertainties in population synthesis model, the emission model and the selection effects. Furthermore it shows that many more short period AM CVn systems might be detectable only as X-ray sources. Some have periods as short as three minutes. About one third of the X-ray sources is also detectable in the optical band.

4.3 Gravitational waves from short period AM CVn systems

In Nelemans et al. (2001b) we presented a study of the gravitational wave signal from Galactic binaries in which both stars are compact objects. In that study we estimated the contribution of AM CVn systems to the double white dwarf noise background and found that AM CVn systems hardly contribute, even though at frequencies between 0.3 and 1 mHz (periods between 33 and 105 minutes) they outnumber the detached double white dwarfs. This is because at these frequencies their chirp mass has fallen far below that of a typical detached system (see also Hils & Bender 2000). We therefore did not consider them anymore. However at shorter periods, where the number of AM CVn systems is much smaller their chirp mass is similar to that of the detached systems from which they originate.

In Fig. 8 we show the Galactic population of detached double white dwarfs and AM CVn systems that can be resolved by LISA. There are $\sim 11\,000$ resolved double white dwarfs as well as $\sim 11\,000$ resolved AM CVn systems. Their distribution is shown by the grey shading. The 200 strongest sources of each type are shown as dots to enhance their visibility. Figure 8 clearly shows that AM CVn systems may be important sources for LISA. Compared to our previous study the ‘confusion limit’, i.e. the frequency at which the unresolved background disappears (see Nelemans et al. (2001b) for details) moves to slightly higher frequency because in our current model there are 213 million detached close double

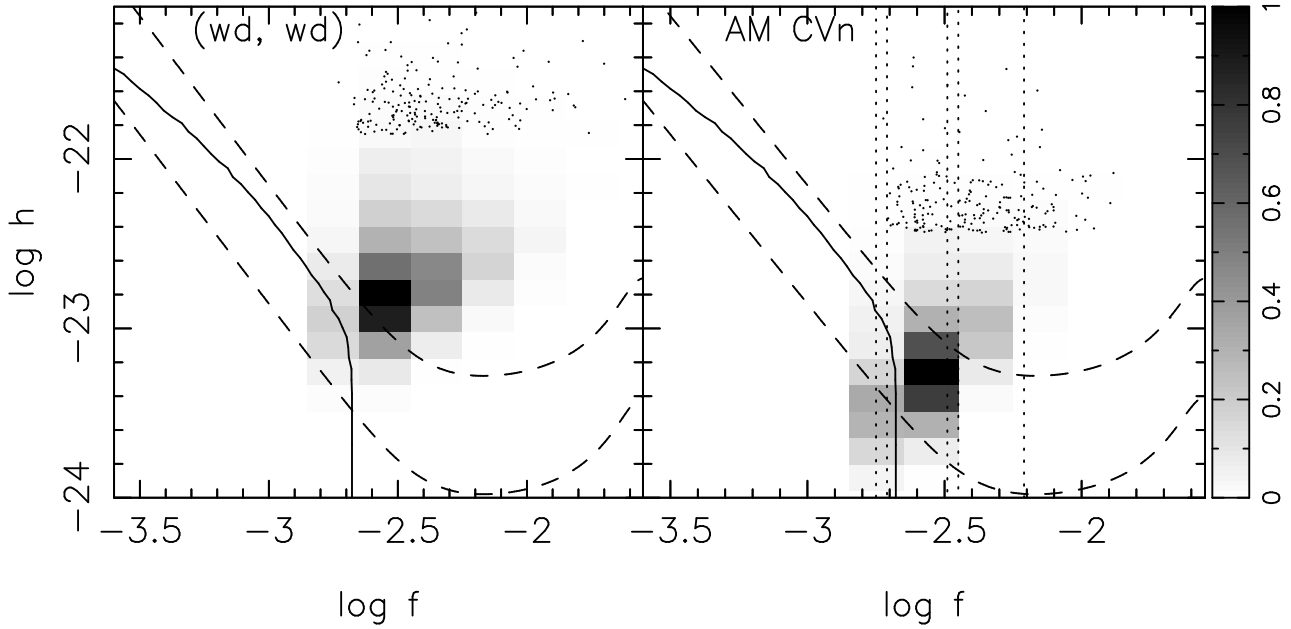


Figure 8. Gravitational wave amplitude h as function of the frequency of the wave for the resolved double white dwarfs (left panel, 10697 objects) and AM CVn systems (right panel, 11000 objects.). The grey shades give the density distribution of the resolved systems normalised to the maximum density in each panel (1548 and 1823 for the double white dwarf and AM CVn panel respectively). The 200 strongest sources in each sample are shown as the dots to enhance their visibility. In the AM CVn panel the periods of the observed short period systems are indicated by the vertical dotted lines. Solid line shows the average background noise due to detached white dwarfs as in Nelemans et al. (2001b). The *LISA* sensitivities for a integration time of one year and a signal-to-noise ratio of 1 and 5 are indicated by the dashed lines (Larson et al. 2000).

white dwarfs, instead of 110 million before, due to the use of different IMF, Galactic model and the changes in stellar evolution.

The crucial difference between AM CVn systems and detached double white dwarfs in the short period range is the sign of their period derivatives. The periods of AM CVn systems increase due to mass transfer, while the periods of detached systems decrease due to GW losses⁵. Assuming conservative mass transfer, the change of the GW frequency ($f = 2/P$) of AM CVn systems formed from double white dwarfs can be derived from

$$\frac{\dot{f}}{f} = -\frac{\dot{P}}{P} = -\frac{3}{2} \frac{\dot{a}}{a} = -3 \frac{\dot{J}_{\text{GWR}}}{J_{\text{orb}}} - 3(1-q) \frac{\dot{m}}{m}, \quad (11)$$

where m is the mass of the donor star and $q = m/M$. We can use the equilibrium mass transfer rate as derived in Marsh et al. (2003) to get

$$\dot{f} = -5.8 \times 10^{-7} f^{11/3} \left(\frac{M}{M_{\odot}} \right)^{5/3} \left(\frac{\zeta_{r_L} - \zeta_2}{2 + \zeta_2 - \zeta_{r_L} - 2q} \right) \text{Hz s}^{-1}, \quad (12)$$

where ζ_2 is the logarithmic derivative of the secondary radius with respect to mass and $\zeta_{r_L} = d \ln(R_L/a)/d \ln m \approx 1/3$ (see Marsh et al. 2003). We wrote the equation in the same form as the corresponding equation for frequency change in detached systems (e.g. Eq. (6) in Nelemans et al. 2001b), with the (positive) term in parentheses giving the change with respect to the detached case. This term is of order unity at the onset of the mass transfer (i.e.

⁵ Note that systems formed from helium stars and evolved secondaries in CVs have decreasing periods before they reach their period minimum (e.g. Tutukov & Fedorova 1989; Podsiadlowski et al. 2003). However, in this phase they are (much) brighter than after the period minimum and are not consistent with being classified as “classical” AM CVn systems.

at highest frequency, above ~ 5 mHz), decreasing to about 0.1 at 2 mHz.

LISA will be able to measure the frequency change of a number of the resolved binaries. In Nelemans et al. (2001b) we estimated the number of systems for which this can be done by requiring that in the course of the experiment the frequency would change by one frequency bin. However, it really is the phase shift resulting from a frequency change that will be measured (e.g. Webbink & Han 1998), so the requirement has to be that over the course of the experiment the phase shifts by a certain amount, compared to a system without frequency change. Writing the phase as an expansion in f , \dot{f} and \ddot{f} , this means \dot{f} can be measured if

$$\Delta\Phi = \dot{f} \frac{T^2}{2} > \Delta\Phi_{\text{min}}, \quad (13)$$

where $\Delta\Phi_{\text{min}}$ is the minimum phase shift that can be measured and T is the duration of the experiment. Analogously \ddot{f} can be measured if

$$\Delta\Phi = \ddot{f} \frac{T^3}{3} > \Delta\Phi_{\text{min}}. \quad (14)$$

Measuring the frequency change provides important information, as the chirp mass can be measured directly for the detached systems. Combined with the wave amplitude h [Eq. (7)], this yields the distance. For AM CVn systems this argument does not hold, as \dot{f} is determined by the mass transfer [Eq. (12)]. However, for an assumed mass–radius relation of the donor star, both the model mass transfer rate and the mass of the donor star (and thus the chirp mass of the system to within a factor of ~ 2) as function of period are fixed (e.g. Vila 1971; Faulkner 1971). Thus a measurement of \dot{f} can test mass–radius models, which is especially interesting because more realistic mass–radius relations for low-mass white dwarfs become available (e.g. Bildsten 2002). In Table 2 we show

$\Delta\Phi_{\min}$	Detached systems		AM CVn systems	
	\dot{f}	\ddot{f}	\dot{f}	\ddot{f}
$\pi/2$	145	0	9	0
$\pi/4$	313	0	22	0
$\pi/8$	636	1	56	0
$\pi/16$	1163	1	108	0
$\pi/32$	1935	2	201	0
$\pi/32, T = 5 \text{ yr}$	10094	23	3416	0

Table 2. Number of systems for which \dot{f} or \ddot{f} can be measured as function of the minimum phase shift needed for detection. The duration of the *LISA* mission is assumed to be 1 year, except for the last row, where a mission time of 5 yr is assumed.

the number of systems for which we can measure the frequency change as function of the minimum phase shift.

Finally it would be very interesting to measure the second derivative of the frequency, as that gives a direct check whether the change in frequency is due to GWR only, or whether other effects (like tidal torques etc.) are important (Webbink & Han 1998, Phinney, private communication). For pure GW losses we have⁶

$$\ddot{f} = \frac{11}{3} \frac{\dot{f}^2}{f}. \quad (15)$$

As can be seen from Table 2, the number of systems for which the second derivative can be measured is small, even for a more optimistic assumption of a total *LISA* operation time of 5 yr. For none of the AM CVn systems we expect its second derivatives to be measurable. This is due to the fact that the AM CVn systems form from pairs of low-mass ($M \lesssim 0.5M_{\odot}$) white dwarfs (e.g. Nelemans et al. 2001a) which have larger radii and thus do not penetrate into the highest frequency range where \ddot{f} is large (see Fig. 8). In this range there are only massive ($M > 1M_{\odot}$) detached double white dwarf pairs that merge rather than become AM CVn systems.

5 RESULTS II: SHORT-PERIOD AM CVn SYSTEMS DETECTABLE BY *LISA* WITH OPTICAL AND/OR X-RAY COUNTERPARTS

In Figure 9 we show the number distributions vs. orbital periods for *LISA* sources that have optical and/or X-ray counterparts, direct impact systems that are GWR and X-ray sources, and the total number of systems that are optical and/or X-ray sources (see also Table 3). For comparison, we indicate also the distribution of the total number of AM CVn systems with $P < 1500$ s as the white histogram in each panel. The systems with different properties are marked by different hatching styles. We will discuss these groups now in more detail.

Resolved *LISA* sources (GWR)

The top left panel shows the 11,000 systems that are expected to be resolved by *LISA* (grey histogram, also shown in Fig. 8), most of which do not have optical or X-ray counterparts. There are 151 short-period systems that have X-ray counterparts (GWR+X) and 143 systems, mainly with periods between 500 and 1000 s, that

have optical counterparts (GWR + Opt). Only 31 systems have both optical and X-ray counterparts (GWR + Opt + X).

Direct impact accretors

The top right panel shows the 2680 systems that are in the direct impact phase of accretion (grey histogram, as in Fig. 4). Most of these systems (2057) are expected to be resolved by *LISA* [DI (GWR)], while at the shortest periods there are 105 X-ray systems that are in the direct impact phase [DI (X)].

Optical sources

The bottom left panel shows (in grey) that for periods below 25 minutes there are 1336 systems that have $V < 20$ mag (grey histogram). These are the systems shown in the bottom panel of Fig. 7, and are the local population of AM CVn systems. Some (106) of these systems are also X-ray systems (Opt + X) and are shown as the filled symbols in the top panel of Fig. 7. Many of the short period systems will show eclipses (even more than the detached systems which are discussed in Cooray et al. 2003) which would compliment the GWR data and provide information on the radii of the components and the inclinations of the systems. E.g. a crude estimate for a typical system with initial parameters $0.25 + 0.6M_{\odot}$ gives a probability for eclipsing the accreting star of about 30 per cent at $P = 1000$ s, and even higher for eclipsing (part of) the accretion disc.

X-ray sources

Finally, the bottom right panel shows the 326 X-ray sources that are also shown in the top panel of Fig. 7. The majority is only detectable in X-rays and many are in the direct impact phase. Only a few direct impact systems are detectable in the optical band, by the radiation from the cooling white dwarf (the filled circles in Fig. 7). At longer periods we expect detectable X-ray emission from the boundary layers of systems formed from helium stars, some of which are also detectable in the *V*-band (Opt + X). These X-ray sources in the *ROSAT* band in our model are concentrated in the Galactic plane, especially towards the Galactic centre. There are 193 systems (60 per cent of the total) in an area between Galactic longitudes -50 and $+50$ degrees and Galactic latitude between -10 and $+10$ degrees. The *ROSAT* all-sky survey⁷ found ~ 4500 sources in this region, so the short-period AM CVn systems can only account for a small fraction of these sources.

It is clear from Fig. 9 that *LISA* is expected to be very effective in detecting the short-period AM CVn systems. A large fraction of these will be in the direct impact phase. At short periods, a significant fraction of the *LISA* sources might be detectable in X-rays, while at longer periods a small fraction might be optical sources.

LISA sources with optical and/or X-ray counterparts are important, as *LISA* will measure a combination of all the parameters that determine the GWR signal (frequency, chirp mass, distance, position in the sky and inclination angle, e.g. Hellings 2003), so if some of these parameters (period, position) can be obtained from optical or X-ray observations the other parameters can be determined with higher accuracy. This is particularly interesting for the distances, inclinations and masses of the systems, which are very difficult to measure with other methods.

6 DISCUSSION

We stress here that AM CVn systems form from binaries with a rather small range of initial parameters and thus that their birth

⁶ Note that Webbink & Han (1998) give 5/3 as numerical factor, which is appropriate for the corresponding equation for the second derivative of the orbital period.

⁷ <http://www.xray.mpe.mpg.de/rosat/survey/rass-fsc/>

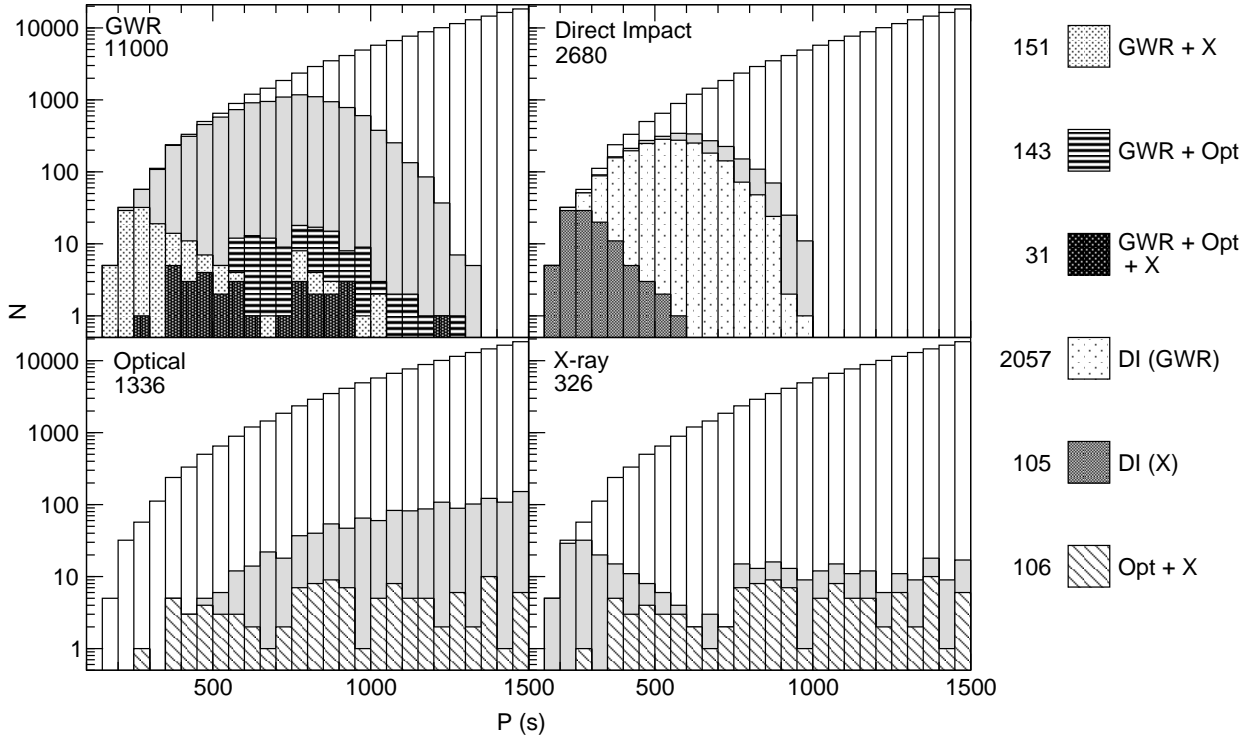


Figure 9. Histograms of the population of short-period AM CVn systems, subdivided in different types. In each panel we show the *total* AM CVn population as the white histogram. In the top left panel we show the systems that can be resolved by *LISA* in grey and subdivide these in the ones that have optical counterparts (GWR + Opt), X-ray counterparts (GWR + X) and both (GWR + Opt + X). Similarly the top right panel shows the population that is in the direct impact phase of accretion in grey and we subdivide that population in GWR and X-ray sources. The bottom two panels show (again in grey) the populations that are detectable in the optical band (left panel) and the X-ray band (right panel). The distribution of sources detectable in both the optical and X-ray band is shown by the hatched histogram in both lower panels (Opt + X). See also Table 3.

	total number	in direct impact phase
AM CVn	138679	2680
GWR	11000	2057
Optical	1336	7
X-ray	326	105
GWR+Opt	143	3
GWR+X	151	103
GWR+Opt+X	31	3
Opt+X	106	3

Table 3. The number of short period ($P < 1500$ s) AM CVn systems with different properties. The number of systems with each property that is in the direct impact phase is given in the second column. See also Fig. 9 for the distribution of these systems over orbital period.

rate is very sensitive to small changes in assumptions in binary population synthesis calculations. One has to keep in mind that a lot of these assumptions are badly constrained, which means that the number of progenitor systems is rather uncertain (e.g. Nelemans et al. 2001c). On top of that, there are uncertainties connected with the formation of AM CVn systems from their immediate progenitors as discussed in Sect. 2.1 and NPVY, making the AM CVn birth rates uncertain by at least an order of magnitude. The models we use for the X-ray and optical emission are very

simplified as well. The interstellar absorption model might very well underestimate the X-ray absorption for the systems in the Galactic centre, which comprise a large fraction of the systems that are detectable only in X-rays (pluses in Fig. 7). We furthermore recall that a number of (possibly important) effects like irradiation and compressional heating are not taken into account in our simple emission models.

For comparison we also computed the results for X-ray detectors sensitive in the range 0.1 – 15 keV (similar to the *Chandra* and *XMM* bands). Because most of our spectra are rather soft, the flux (\mathcal{F}) in this band is generally not much larger than in the *ROSAT* band: 80 per cent has $\mathcal{F}_{\text{XMM}}/\mathcal{F}_{\text{ROSAT}} < 1.5$; 96 per cent has $\mathcal{F}_{\text{XMM}}/\mathcal{F}_{\text{ROSAT}} < 3$. However, the improved sensitivity of *Chandra* and *XMM* obviously will have an impact. For instance the Munro et al. (2003) *Chandra* observations of the Galactic Centre have a completeness limit of 3×10^{-15} erg cm $^{-2}$ s $^{-1}$, almost two orders of magnitude deeper than our assumed *ROSAT* limit. The number of X-ray sources in the 0.1 – 15 keV band detectable down to 10^{-14} erg cm $^{-2}$ s $^{-1}$ is 644 and 1085 down to 10^{-15} erg cm $^{-2}$ s $^{-1}$. In the *Chandra* mosaic image of the Galactic centre (Wang et al. 2002), roughly down to 10^{-14} erg cm $^{-2}$ s $^{-1}$ there are ~ 1000 point sources, while our model gives 16 X-ray systems in this region. In the tiny Munro et al. (2003) region, where they identify more than 2000 sources, we predict 3 AM CVn systems with X-ray flux above 10^{-15} erg cm $^{-2}$ s $^{-1}$.

As briefly discussed in Sect. 2, we did not include AM CVn systems formed like CVs in our models. The reason is that for the production of the short period systems, which we consider in this paper, this channel is not effective. An evolutionary track for a donor with an initial mass of $0.96 M_{\odot}$ and a hydrogen-exhausted core $\sim 0.05 M_{\odot}$ (sequence nr. 4 in Fedorova & Ergma 1989) reaches a minimum period of 8.4 minutes and spends $3.8 \cdot 10^7$ yr in the 25 – 8.4 minute period range (A.V. Fedorova, private communication). Taking this time as typical, and assuming a birth rate of $6.4 \cdot 10^{-5} \text{ yr}^{-1}$ for systems evolving to $P < 25$ minutes, as in the standard model of Podsiadlowski et al. (2003), we expect 2400 post-CV ultra-compact systems in the Galaxy, compared to the 140,000 from the channels discussed here. However, if these channels are ineffective, e.g., due to the instability of the mass transfer and/or destruction of accretors by edge-lit detonations (NPVY), the AM CVn systems from CVs may become more important even at short periods.

7 CONCLUSION

We discussed a model for the Galactic population of short-period AM CVn systems and the uncertainties in this model. We find a total population of AM CVn systems in the Galaxy with periods shorter than 1500 s of $\sim 140,000$ systems. We estimate that the final uncertainty on this number is at least a factor of 10. The model presented here gives an optimistic estimate of the total number of systems, i.e. all quoted numbers could be (substantially) smaller. We calculated the optical, X-ray and gravitational wave signals that could be detectable, using simple emission models and selection effects, and discussed the overlap between the subpopulations which may be discovered by different detection methods.

In this optimistic model we find that there are a few systems expected that are in the direct impact phase and are detectable as optical and X-ray sources, where the optical emission comes from the cooling of the (possibly heated) white dwarfs. Thus if RX J0806 and V407 Vul turn out to be short period AM CVn systems, that would argue for an optimistic model as in a pessimistic model there would be no such systems that are observable. Strohmayer (2002) and Hakala et al. (2003) have reported a shortening of the periods in V407 Vul and RX J0826, arguing against this interpretation despite the fact that these stars might be helium-donor or CV systems before the period minimum (see also Woudt & Warner (2003a) who argue that there is not sufficient evidence for a shortening of the period in RX J0806).

At the observed periods of RX J0806, V407 Vul and ES Cet, the fraction of systems that is in the direct impact phase is 80, 40 and 30 per cent respectively. The total number of direct impact systems in the Galaxy is 2680. We further find that there are 220 (very) short period AM CVn systems that are only detectable in the X-ray band, some with orbital periods as short as 3 minutes.

We conclude that the future gravitational wave detector *LISA* is expected to discover thousands of short-period AM CVn systems, about ten per cent of the total number of short-period systems in the Galaxy. The number of systems with periods below 1500 s that is detectable in the optical band is 1336 (about one per cent of the total). Only 326 systems (0.25 per cent) are detectable in the ROSAT X-ray band. For the typical sensitivities of *Chandra* and XMM, the number of detectable sources over the whole sky is $\gtrsim 1000$, still only a tiny fraction of all X-ray sources.

For many of the *LISA* sources the change in frequency can be measured, which would provide a test of the mass – radius rela-

tion for the donor stars in these systems. *LISA* is expected to detect a similar number of detached double white dwarfs, for many of which the frequency change can be determined, yielding a direct measurement of the distances to these sources. Maybe for a few the second derivative of the frequency can be measured, which would give a direct test whether the frequency change is purely due to GWR, or whether tidal effects play a role.

Our results indicate that many short-period AM CVn systems may be detectable in more than one way. A total of 106 systems is detectable in the optical and X-ray bands. For the systems that are detectable with *LISA*, about 300 (3 per cent) have optical and/or X-ray counterparts, giving the opportunity to independently determine the position and orbital period. This leads to a better determination of the other parameters that can be derived from the GWR signal (i.e. inclination and masses) and would lead to unprecedented accuracy in the study of these extreme binaries.

ACKNOWLEDGMENTS

We thank the referee for comments that improved the paper. We thank Samuel Boissier for providing the table of star formation rates and helpful discussion about the Galactic model. GN is supported by PPARC. LRY is supported by RFBR grant no. 03-02-16254 and Federal Science and Technology Program “Astronomy” (contract no. 40.022.11.1102). SPZ is supported by the KNAW and NWO.

REFERENCES

- Bath G.T., Evans W.D., Papaloizou J., Pringle J.E., 1974, MNRAS, 169, 447
- Bildsten L., 2002, ApJ, 577, L27
- Boissier S., Prantzos N., 1999, MNRAS, 307, 857
- Cooray A., Farmer A.J., Seto N., 2003, ApJ, submitted, astro-ph/0310889
- Cropper M., Harrop-Allin M.K., Mason K.O., et al., 1998, MNRAS, 293, L57
- Driebe T., Schönberner D., Blöcker T., Herwig F., 1998, A&A, 339, 123
- Evans C.R., Iben I. Jr, Smarr L., 1987, ApJ, 323, 129
- Faulkner J., 1971, ApJ, 170, L99
- Fedorova A.V., Ergma E.V., 1989, Ap&SS, 151, 125
- Hakala P., Ramsay G., Wu K., et al., 2003, MNRAS, 343, 10
- Han Z., Webbink R.F., 1999, A&A, 349, L17
- Hansen B.M.S., 1999, ApJ, 520, 680
- Hellings R.W., 2003, Class. Quantum Grav., 20, 1019
- Hils D., Bender P.L., 2000, ApJ, 537, 334
- Hoare M.G., Drew J.E., 1991, MNRAS, 249, 452
- Hurley J.R., Pols O.R., Tout C.A., 2000, MNRAS, 315, 543
- Iben I. Jr, Tutukov A.V., Fedorova A.V., 1998, ApJ, 503, 344
- Israel G.L., Panzera M.R., Campana S., et al., 1999, A&A, 349, L1
- Israel G.L., Hummel W., Covino S., et al., 2002, A&A, 386, L13
- Jha S., Garnavich P., Challis P., Kirshner R., Berlind P., 1998, IAU Circ., 6983
- Kato M., Hachisu I., 1999, ApJ, 513, L41
- Kippenhahn R., Meyer-Hofmeister E., 1977, A&A, 54, 539
- Klypin A., Zhao H., Somerville R.S., 2002, ApJ, 573, 597
- Kroupa P., Tout C.A., Gilmore G., 1993, MNRAS, 262, 545

Larson S.L., Hiscock W.A., Hellings R.W., 2000, *Phys. Rev. D*, 62, 062001

Marsh T., Nelemans G., Steeghs D., 2003, submitted to *MNRAS*, Marsh T.R., Steeghs D., 2002, *MNRAS*, 331, L7

Mauche C.W., Wade R.A., Polidan R.S., van der Woerd H., Paerels F.B.S., 1991, *ApJ*, 372, 659

Miller G.E., Scalo J.M., 1979, *ApJS*, 41, 513

Morrison R., McCammon D., 1983, *ApJ*, 270, 119

Motch C., Haberl F., Guillout P., et al., 1996, *A&A*, 307, 459

Muno M.P., Baganoff F.K., Bautz M.W., et al., 2003, *ApJ*, 589, 225

Nelemans G., Verbunt F., Yungelson L.R., Portegies Zwart S.F., 2000, *A&A*, 360, 1011

Nelemans G., Portegies Zwart S.F., Verbunt F., Yungelson L.R., 2001a, *A&A*, 368, 939

Nelemans G., Yungelson L.R., Portegies Zwart S.F., 2001b, *A&A*, 375, 890

Nelemans G., Yungelson L.R., Portegies Zwart S.F., Verbunt F., 2001c, *A&A*, 365, 491

Norton A.J., Haswell C.A., Wynn G.A., 2002, submitted to *MNRAS*, preprint (astro-ph/0206013)

Paczynski B., 1967, *Acta Astron.*, 17, 287

Podsiadlowski P., Han Z., Rappaport S., 2003, *MNRAS*, 340, 1214

Pols O.R., Marinus M., 1994, *A&A*, 288, 475

Portegies Zwart S.F., Verbunt F., 1996, *A&A*, 309, 179

Predehl P., Schmitt J.H.M.M., 1995, *A&A*, 293, 889

Pringle J.E., 1977, *MNRAS*, 178, 195

Pringle J.E., 1988, *MNRAS*, 230, 587

Ramsay G., Cropper M., Wu K., Mason K.O., Hakala P., 2000, *MNRAS*, 311, 75

Ramsay G., Hakala P., Cropper M., 2002a, *MNRAS*, 332, L7

Ramsay G., Wu K., Cropper M., et al., 2002b, *MNRAS*, 333, 575

Rezzolla L., Uryu K., Yoshida S., 2001, *MNRAS*, 327, 888

Ruiz M.T., Rojo P.M., Garay G., Maza J., 2001, *ApJ*, 552, 679

Sandage A., 1972, *ApJ*, 178, 1

Solheim J.E., 2003, in de Martino D., Silvotti R., Solheim J.E., Kalytis R., eds., *White Dwarfs*, volume 105 of *NATO Science Series II – Mathematics, Physics and Chemistry*, Kluwer, p. 299

Strohmayer T.E., 2002, *ApJ*, 581, 577

Thorstensen J.R., 2003, *ApJ*, in press, astro-ph/0308516

Townsend D.M., Bildsten L., 2002, *ApJ*, 565, L35

Tsugawa M., Osaki Y., 1997, *PASJ*, 49, 75

Tutukov A.V., Fedorova A.V., 1989, *SvA*, 33, 606

Tutukov A.V., Yungelson L.R., 1996, *MNRAS*, 280, 1035

Tutukov A.V., Fedorova A.V., Ergma E.V., Yungelson L.R., 1987, *SvAL*, 13, 328

Ulla A., 1995, *A&A*, 301, 469

van Teeseling A., Verbunt F., 1994, *A&A*, 292, 519

van Teeseling A., Beuermann K., Verbunt F., 1996, *A&A*, 315, 467

Verbunt F., Rappaport S., 1988, *ApJ*, 332, 193

Vila S.C., 1971, *ApJ*, 168, 217

Wade R.A., 1984, *MNRAS*, 208, 381

Wang Q.D., Gottlieb E.V., Lang C.C., 2002, *Nature*, 415, 148

Warner B., 1995, *Ap&SS*, 225, 249

Warner B., Woudt P.A., 2002, *PASP*, 114, 129

Webbink R.F., 1984, *ApJ*, 277, 355

Webbink R.F., Han Z., 1998, in *Laser Interferometer Space Antenna*, number 456 in *AIP Conf. Proc.*, AIP, New York, p. 61

Wood M.A., Casey M.J., Garnavich P.M., Haag B., 2002, *MNRAS*, 334, 87

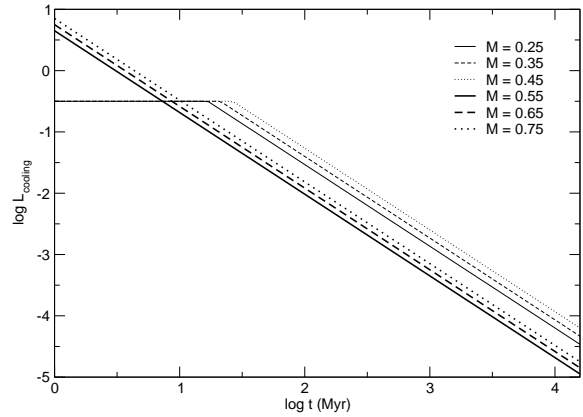


Figure A1. Cooling curves of white dwarfs used in this paper. The curves are a rough translation of Fig. 10 of Hansen (1999).

Woudt P.A., Warner B., 2003a, in *White Dwarfs: Galactic and Cosmological Probes*, proceedings of IAU JD5, astro-ph/0310494

Woudt P.A., Warner B., 2003b, *MNRAS*, in press, astro-ph/0307473

Wu K., Cropper M., Ramsay G., Sekiguchi K., 2002, *MNRAS*, 331, 221

Yoon S.C., Langer N., 2003, in Maeder A., Eenens P., eds., *Stellar Rotation*, IAU-Symp 215, ASP, San Francisco

Zapolsky H.S., Salpeter E.E., 1969, *ApJ*, 158, 809

APPENDIX A: WHITE DWARF COOLING

We model the cooling of white dwarf based on the curves of Hansen (1999). We abandoned the previous use of the Driebe et al. (1998) models, since their models with thick hydrogen envelopes cool slower than observations of detached double white dwarfs suggest and their thick hydrogen envelopes actually may be lost in hydrogen shell flashes (e.g. Nelemans et al. 2001c).

Our simple models have carbon-oxygen white dwarfs that cool faster than helium white dwarfs, but within the groups the most massive objects are brighter at given age. We model the curves as (see Fig. A1):

$$\log L = L_{\max} - 1.33 \log(t/10^6 \text{ yr}), \quad (\text{A1})$$

where L_{\max} is a linear fit given by

$$L_{\max} = 1 - (0.9 - M_{\text{WD}}) \quad \text{for } M_{\text{WD}} > 0.5 M_{\odot}, \quad (\text{A2})$$

and

$$L_{\max} = 1.4 - 1.33(0.45 - M_{\text{WD}}) \quad \text{for } M_{\text{WD}} < 0.5 M_{\odot} \quad (\text{A3})$$

(mass and luminosity in solar units). For white dwarf masses below $0.5 M_{\odot}$ the luminosity is constrained to be below $\log L/L_{\odot} = -0.5$, for more massive white dwarfs below $\log L/L_{\odot} = 2$.